

Modeling the Effect of Cross-Link Density on Resins Catalytic Activities

Leandro G. Aguiar,* William M. Godoy, Leonardo Nápolis, Rui P. V. Faria, and Alírio E. Rodrigues

Cite This: <https://doi.org/10.1021/acs.iecr.1c00695>

Read Online

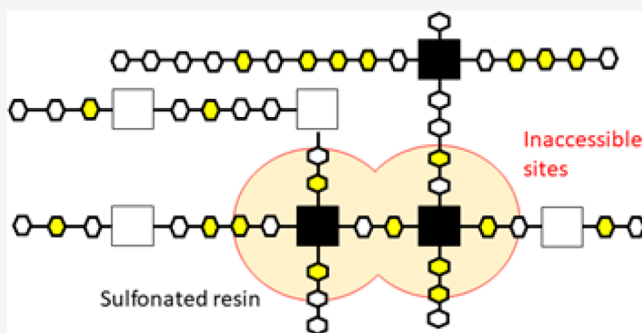
ACCESS |

Metrics & More

Article Recommendations

Supporting Information

ABSTRACT: Two mathematical models were coupled to quantitatively assess the effect of cross-link density on the catalytic activity of sulfonated styrene–divinylbenzene (DVB) resins: (I) a copolymerization model comprised of the mass balances of species and sequences, which is used to quantify inaccessible catalytic sites, and (II) a second-order pseudohomogeneous kinetic model to describe the catalyzed reactions. The fraction of inaccessible sites ranged from 10% to 72% of the total sites for resins with 4% and 20% DVB, respectively. It was found that chain segments with six or less monomer units between cross-links contain inaccessible sites for the catalyzed reactions studied herein. The mathematical approach was validated with 53 catalysis experiments from the literature and provided good agreements. A linear correlation for the fraction of inaccessible sites was proposed and validated, providing $R^2 = 0.992$. These results can represent a valuable tool to improve the performance of styrene–DVB-based catalysts.



1. INTRODUCTION

Ion exchange resins have been applied as catalysts in different organic reactions over the past decades. Most of these resins consist of a polymer network containing divinylbenzene (DVB) as the cross-linker and styrene as the vinyl monomer. What gives the ion exchange character to the resin is the sulfonic groups attached to the styrene aromatic rings. Playing a catalytic role in many reactions, sulfonated styrene–DVB resins from commercial lines such as Amberlyst,¹ Amberlite,² Purolite,^{3,4} Dowex,⁵ and Lewatit,⁶ among others, have been extensively studied. Recently, modified resins composed of styrene cross-linked with alternative divinyl monomers such as ethylene glycol dimethacrylate (EGDMA) and triethylene glycol dimethacrylate (TEGDMA) have been synthesized and tested in esterification reactions.^{7–9} These resins presented promising catalytic activity, indicating that the properties of the polymer matrix and the consequent accessibility to catalytic sites should be better explored. The catalytic efficiency of sulfonated resins depends not only on their porosity, specific surface, and ion exchange capacity but also on their degree of cross-linking and consequent swelling indexes. Historically, some attempts to correlate the resin's degree of cross-linking with its efficiency in catalysis have been conducted by different approaches such as the synthesis and application of resins with different textural properties,¹⁰ experimental study of commercial ion exchange resins differed markedly in their polymer structure,¹¹ and development of an empirical equation which takes into account the contribution of each individual fraction of swollen polymer to the overall rate of catalyzed reactions.⁴ Conversely, a phenomenological approach

for the fraction of inaccessible sites as a function of sequences involving a mathematical characterization of the polymer network and the use of this information in the catalytic process constitutes a novelty. One can assert that the matrix properties are a result of the polymerization conditions such as temperature, dilution degree, and cross-linker content, among others. Modeling approaches for copolymerization can provide a description of the resin formation and its characteristics at a molecular level.^{12–14} Information such as molecular weight between cross-links and entrapped pendant double bounds can be estimated by this kind of mathematical model.¹⁵

The present study proposes a modeling approach to quantify inaccessible catalytic sites in acidic resins as a function of their polymer network structure and to assess this accessibility effect on catalyzed reactions (mostly esterifications). For this purpose, two specific objectives were defined: (I) to simulate the resin production through a copolymerization model in order to obtain information about the resin structure; (II) to collect the main data, from the copolymerization model, concerning the accessibility through the matrix and use this data in the modeling of resin-catalyzed reactions.

The present study proposes a modeling approach to quantify inaccessible catalytic sites in acidic resins as a function of their polymer network structure and to assess this accessibility effect on catalyzed reactions (mostly esterifications). For this purpose, two specific objectives were defined: (I) to simulate the resin production through a copolymerization model in order to obtain information about the resin structure; (II) to collect the main data, from the copolymerization model, concerning the accessibility through the matrix and use this data in the modeling of resin-catalyzed reactions.

Received: February 16, 2021

Revised: April 8, 2021

Accepted: April 8, 2021

2. MODELING

The mathematical approach developed in the present study aims to establish a connection between the resin production model and resin-catalyzed reaction model. All the symbols used in their description are defined in the symbology section.

2.1. Copolymerization Model. The mathematical model conceived herein consists of the description of a vinyl/divinyl free-radical copolymerization. Since most of sulfonated resins are made of styrene cross-linked with divinylbenzene (DVB), this copolymerization system, initiated with benzoyl peroxide (BPO), was considered in the present work. Table 1 relates the copolymerization steps used in the system description.¹⁵

Table 1. Copolymerization Steps^a

reaction	chemical equation
initiator decomposition	$I \xrightarrow{k_d} 2R_0$
initiation	$R_0 + M_j \xrightarrow{k_{tj}} R \quad j = 1, 2$
PDB initiation	$R_0 + PDB \xrightarrow{k_{p3}} R$
monomer propagation	$R + M_j \xrightarrow{k_{pj}} R \quad j = 1, 2$
PDB propagation	$R + PDB \xrightarrow{k_{p3}} R$
termination by combination	$R + R \xrightarrow{k_t} P$

^aI: initiator, R₀: primary radical, M_j: monomer of type j, R: polymeric radical, PDB: pendent double bond, P: dead polymer, k_d to k_t: rate constants of the reactions.

The polymeric radical R represents the group of all possible polymer radicals in the media (from styrene, DVB and PDB). It is well-known that different radicals have different reactivities. Nonetheless, these reactivities were taken into account in the model by calculating average rate constants, as described in the Results and Discussion section.

Sulfonated styrene–DVB resins from commercial lines such as Amberlyst and Dowex present sulfonic groups (SO₃H) which are functional in applications such as ion exchange and catalysis. The ion exchange capacity (IEC) of a sulfonated resin is defined

as the mmol (or mequiv) of SO₃H per gram of resin. When this material is applied as a catalyst, the IEC can be understood as the content of catalytic sites. There are several types of sulfonated resins with different cross-linking densities due to the variety of DVB percentage in their composition,¹⁶ i.e., the greater the DVB content, the greater the cross-linking degree. In this sense, when analyzing the effect of cross-linking density on the catalytic activity of the resins, a higher hindering effect (inaccessible catalytic sites) is expected in resins with higher DVB percentage. The present model describes an attempt to identify regions in the polymer network which are likely to be inaccessible when conducting a reaction catalyzed by a given resin. It is proposed that these inaccessible regions occur around two cross-linked units connected by a sequence of *n* repeating units, this sequence was named L_{En}. It is understood that smaller L_{En} sequences can cause higher number of entanglements due to the proximity of the chains. Then, a maximum number of repeating units, *n_i*, was defined as a condition for inaccessibility, i.e., hindering effect occurs in L_{En} only for *n* ≤ *n_i*. This approach provides a correlation between the cross-linking degree of the resin and the possible inaccessible sites. In order to model the sequences formation in the resin, the copolymerization kinetics were studied in terms of sequences, as defined in Figure 1.

Figure 1 also illustrates the inaccessible regions considered due to the proximity of two cross-linked units. It is understood that the inaccessibility of a molecule to a given region in the polymer matrix depends on the size of this molecule. In general, sulfonating agents are small molecules¹⁷ which can access more sites than molecules involved in a catalyzed reaction (e.g., esterification). Hence, it was considered that sulfonated units are equally distributed along the polymer matrix regardless of the entanglement degree.

The copolymerization reactions in terms of sequences are presented in Table 2 (subindexes *r* and *s* represent repeating units, same as *n* in Figure 1).

The assumptions considered in the copolymerization model are

1. The sequences distributions are considered to be the same in soluble and gel polymer (gelation was not modeled);
2. Cyclization reactions were neglected;

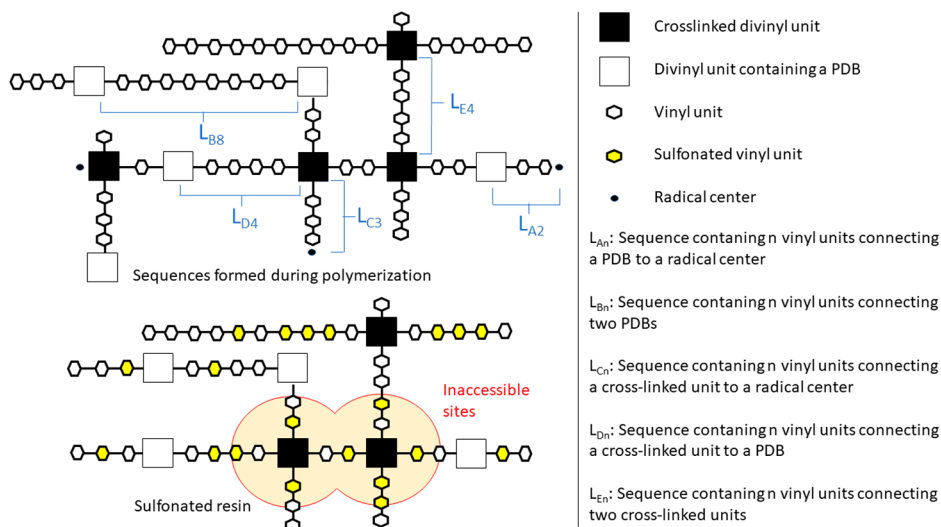


Figure 1. Sequences definition and hindering effect.

Table 2. Reactions in Terms of Sequences^a

chemical equations		
$R_0^\cdot + M_1 \xrightarrow{k_{i1}} R_S^\cdot$	$L_{Ar} + L_{As} \xrightarrow{k_t} L_{Br+s}$	$R_S^\cdot + L_{Ar} \xrightarrow{k_t} F$
$R_S^\cdot + M_1 \xrightarrow{k_{i1}} R_S^\cdot$	$L_{Ar} + L_{Cs} \xrightarrow{k_t} L_{Dr+s}$	$R_S^\cdot + L_{Cr} \xrightarrow{k_t} F$
$R_0^\cdot + M_2 \xrightarrow{k_{i2}} L_{A0}$	$L_{Ar} + L_{As} \xrightarrow{k_{p3}} L_{Cr} + L_{C0}$	$R_S^\cdot + L_{Ar} \xrightarrow{k_{p3}} L_{Cr} + L_{C0}$
$R_S^\cdot + M_2 \xrightarrow{k_{p2}} L_{A0}$	$L_{Ar} + L_{Bs} \xrightarrow{k_{p3}} L_{Dr} + L_{Ds} + L_{C0}$	$R_S^\cdot + L_{Br} \xrightarrow{k_{p3}} L_{Dr} + L_{C0}$
$R_S^\cdot + R_S^\cdot \xrightarrow{k_t} P$	$L_{Ar} + L_{Ds} \xrightarrow{k_{p3}} L_{Dr} + L_{Es} + L_{C0}$	$R_S^\cdot + L_{Dr} \xrightarrow{k_{p3}} L_{Er} + L_{C0}$
$L_{Ar} + M_1 \xrightarrow{k_{p1}} L_{Ar+1}$	$L_{Cr} + L_{As} \xrightarrow{k_{p3}} L_{Er} + L_{Cs} + L_{C0}$	$R_0^\cdot + L_{Ar} \xrightarrow{k_{p3}} L_{Cr} + L_{C0}$
$L_{Ar} + M_2 \xrightarrow{k_{p2}} L_{Br} + L_{A0}$	$L_{Cr} + L_{Bs} \xrightarrow{k_{p3}} L_{Er} + L_{Ds} + L_{C0}$	$R_0^\cdot + L_{Br} \xrightarrow{k_{p3}} L_{Dr} + L_{C0}$
$L_{Cr} + M_1 \xrightarrow{k_{p1}} L_{Cr+1}$	$L_{Cr} + L_{Ds} \xrightarrow{k_{p3}} L_{Er} + L_{Es} + L_{C0}$	$R_0^\cdot + L_{Dr} \xrightarrow{k_{p3}} L_{Er} + L_{C0}$
$L_{Cr} + M_2 \xrightarrow{k_{p2}} L_{Dr} + L_{A0}$	$L_{Cr} + L_{Cs} \xrightarrow{k_t} L_{Er+s}$	

^a R_0^\cdot : primary radical, M_1 : vinyl monomer (styrene), M_2 : divinyl monomer (divinylbenzene—DVB), R_S^\cdot : polymeric radical containing only styrene units, P: dead polymer, F: polymer fragment, L_{Ar} – L_{Er} : sequences containing r repeating units.

3. The distribution of sequences containing only styrene units connecting the extreme groups (L_{An} – L_{En}) is considered to be the same as the distribution containing styrene and/or DVB units;

4. Terminal model.

Concerning the aforementioned assumptions, it is important to point out that, under the studied DVB feedings, the gelation is supposed to occur at the very beginning of the reaction (in general before the first hour);¹⁸ i.e., the soluble fraction is very small during most of the reaction period. Additionally, the reactivity of soluble radicals can be considered the same as the reactivity of radical centers along the gel, without impairing the model predictability. Specifically concerning the modeling of cyclization kinetics, it can be done at the cost of considerable computational effort. However, the effect of considering cyclization in the model, for DVB fed in the range 4–100%, is a small shift in monomer conversion and PDBs concentration profiles,¹⁹ justifying the neglect of this reaction step. Furthermore, only sequences involving DVB/PDB units were assessed since they participate in the cross-linking points. Sequences which do not account for the cross-linking density (e.g., sequences connecting two radical centers) were not assessed. Diffusion effects in the copolymerization were neglected due to the degree of dilution studied (150%).

The balances in terms of species and sequences are written as follows.

2.2. Balance of Species.

$$\frac{dI}{dt} = -k_d I \quad (1)$$

$$\frac{dR_0^\cdot}{dt} = 2fk_d I - k_{i1} R_0^\cdot M_1 - k_{i2} R_0^\cdot M_2 - k_{p3} R_0^\cdot PDB \quad (2)$$

$$\frac{dR^\cdot}{dt} = k_{i1} R_0^\cdot M_1 + k_{i2} R_0^\cdot M_2 - k_t R^{\cdot 2} \quad (3)$$

$$\frac{dPDB}{dt} = k_{i2} R_0^\cdot M_2 + k_{p2} R M_2 - k_{p3} PDB (R_0^\cdot + R) \quad (4)$$

$$\frac{dM_1}{dt} = -k_{i1} R_0^\cdot M_1 - k_{p1} R M_1 \quad (5)$$

$$\frac{dM_2}{dt} = -k_{i2} R_0^\cdot M_2 - k_{p2} R M_2 \quad (6)$$

2.3. Balance of Sequences.

$$\begin{aligned} \frac{dR_S^\cdot}{dt} = & k_{i1} R_0^\cdot M_1 - k_{p2} R_S^\cdot M_2 - k_{p3} R_S^\cdot \left(\sum_{r=0}^{n_{\max}} L_{Ar} + \sum_{r=0}^{n_{\max}} L_{Br} + \right. \\ & \left. \sum_{r=0}^{n_{\max}} L_{Dr} \right) - k_t R_S^\cdot \left(\sum_{r=0}^{n_{\max}} L_{Ar} + \sum_{r=0}^{n_{\max}} L_{Cr} \right) - \frac{1}{2} k_t R_S^{\cdot 2} \end{aligned} \quad (7)$$

$$\begin{aligned} \frac{dL_{A0}}{dt} = & k_{i2} R_0^\cdot M_2 + k_{p2} M_2 \left(\sum_{r=0}^{n_{\max}} L_{Ar} + \sum_{r=0}^{n_{\max}} L_{Cr} + R_S^\cdot \right) - L_{A0} \\ & \left[k_{p1} M_1 + k_{p2} M_2 + k_t \left(\sum_{r=0}^{n_{\max}} L_{Ar} + \sum_{r=0}^{n_{\max}} L_{Cr} + R_0^\cdot + R_S^\cdot \right) \right. \\ & \left. + k_{p3} \left(\sum_{r=0}^{n_{\max}} L_{Ar} + \sum_{r=0}^{n_{\max}} L_{Br} + \sum_{r=0}^{n_{\max}} L_{Dr} + R_0^\cdot + R_S^\cdot \right) \right] \end{aligned} \quad (8)$$

$$\begin{aligned} \frac{dL_{Ar}}{dt} = & k_{p1} M_1 L_{Ar-1} - k_{p1} M_1 L_{Ar} - k_{p2} M_2 L_{Ar} \\ & - k_t L_{Ar} \left(\frac{1}{2} \sum_{s=0}^{n_{\max}} L_{As} + \sum_{s=0}^{n_{\max}} L_{Cs} + R_S^\cdot \right) \\ & - k_{p3} L_{Ar} \left(\sum_{s=0}^{n_{\max}} L_{As} + \sum_{s=0}^{n_{\max}} L_{Bs} + \sum_{s=0}^{n_{\max}} L_{Cs} + \right. \\ & \left. \sum_{s=0}^{n_{\max}} L_{Ds} + R_S^\cdot + R_0^\cdot \right) \end{aligned} \quad (9)$$

$$\frac{dL_{B_0}}{dt} = k_{p_2}L_{A_0}M_2 + \frac{1}{2}k_tL_{A_0}^2 - k_{p_3}L_{B_0}\left(\sum_{r=0}^{n_{\max}}L_{A_r} + \sum_{r=0}^{n_{\max}}L_{C_r} + R_0 + R_S\right) \quad (10)$$

$$\frac{dL_{B_r}}{dt} = k_{p_2}L_{A_r}M_2 + k_t\sum_{s=1}^rL_{A_s}L_{A_{r-s}} - k_{p_3}L_{B_r}\left(\sum_{s=0}^{n_{\max}}L_{A_s} + \sum_{s=0}^{n_{\max}}L_{C_s} + R_0 + R_S\right) \quad (11)$$

$$\begin{aligned} \frac{dL_{C_0}}{dt} = & -k_{p_1}L_{C_0}M_1 - k_{p_2}L_{C_0}M_2 \\ & - k_tL_{C_0}\left(\sum_{s=0}^{n_{\max}}L_{A_s} + \sum_{s=0}^{n_{\max}}L_{C_s} + R_S\right) \\ & - k_{p_3}L_{C_0}\left(\sum_{s=0}^{n_{\max}}L_{A_s} + \sum_{s=0}^{n_{\max}}L_{B_s} + \sum_{s=0}^{n_{\max}}L_{D_s}\right) \\ & + k_{p_3}\sum_{r=0}^{n_{\max}}L_{A_r} \\ & \left(\sum_{r=0}^{n_{\max}}L_{A_s} + \sum_{s=0}^{n_{\max}}L_{B_s} + \sum_{s=0}^{n_{\max}}L_{C_s} + \sum_{s=0}^{n_{\max}}L_{D_s} + R_S + R_0\right) \\ & + k_{p_3}\sum_{r=0}^{n_{\max}}L_{B_r}\left(\sum_{s=0}^{n_{\max}}L_{C_s} + R_S + R_0\right) \\ & + k_{p_3}\sum_{r=0}^{n_{\max}}L_{D_r}\left(\sum_{s=0}^{n_{\max}}L_{C_s} + R_S + R_0\right) \end{aligned} \quad (12)$$

$$\begin{aligned} \frac{dL_{C_r}}{dt} = & k_{p_1}L_{C_{r-1}}M_1 - k_{p_1}L_{C_r}M_1 - k_{p_2}L_{C_r}M_2 \\ & + k_tL_{C_r}\left(\sum_{s=0}^{n_{\max}}L_{A_s} + \sum_{s=0}^{n_{\max}}L_{C_s} + R_S\right) \\ & - k_{p_3}L_{C_r}\left(\sum_{s=0}^{n_{\max}}L_{A_s} + \sum_{s=0}^{n_{\max}}L_{B_s} + \sum_{s=0}^{n_{\max}}L_{D_s}\right) \\ & + k_{p_3}L_{A_r}\left(\sum_{s=0}^{n_{\max}}L_{A_s} + \sum_{s=0}^{n_{\max}}L_{C_s} + R_S + R_0\right) \end{aligned} \quad (13)$$

$$\begin{aligned} \frac{dL_{D_0}}{dt} = & k_{p_2}M_2L_{C_0} + k_tL_{A_0}L_{C_0} \\ & + k_{p_3}L_{A_0}\left(\sum_{s=0}^{n_{\max}}L_{B_s} + \sum_{s=0}^{n_{\max}}L_{D_s}\right) \\ & + k_{p_3}L_{B_0}\left(\sum_{s=0}^{n_{\max}}L_{A_s} + \sum_{s=0}^{n_{\max}}L_{C_s} + R_0 + R_S\right) \\ & - k_{p_3}L_{D_0}\left(\sum_{s=0}^{n_{\max}}L_{A_s} + \sum_{s=0}^{n_{\max}}L_{C_s} + R_0 + R_S\right) \end{aligned} \quad (14)$$

$$\begin{aligned} \frac{dL_{D_r}}{dt} = & k_{p_2}L_{C_r}M_2 + k_t\sum_{s=1}^rL_{A_s}L_{C_{r-s}} \\ & + k_{p_3}L_{A_r}\left(\sum_{s=0}^{n_{\max}}L_{B_s} + \sum_{s=0}^{n_{\max}}L_{D_s}\right) \\ & + k_{p_3}L_{B_r}\left(\sum_{s=0}^{n_{\max}}L_{A_s} + \sum_{s=0}^{n_{\max}}L_{C_s} + R_S + R_0\right) \\ & - k_{p_3}L_{D_r}\left(\sum_{s=0}^{n_{\max}}L_{A_s} + \sum_{s=0}^{n_{\max}}L_{C_s} + R_S + R_0\right) \end{aligned} \quad (15)$$

$$\begin{aligned} \frac{dL_{E_0}}{dt} = & k_{p_3}L_{A_s}(L_{C_0} + L_{D_0}) + k_{p_3}L_{C_0}\left(\sum_{s=0}^{n_{\max}}L_{B_s} + \sum_{s=0}^{n_{\max}}L_{D_s}\right) \\ & + k_{p_3}L_{D_0}\left(\sum_{s=0}^{n_{\max}}L_{C_s} + R_0 + R_S\right) + \frac{1}{2}k_tL_{C_0}^2 \end{aligned} \quad (16)$$

$$\begin{aligned} \frac{dL_{E_r}}{dt} = & k_{p_3}\sum_{s=0}^{n_{\max}}L_{A_s}(L_{C_r} + L_{D_r}) + k_{p_3}L_{C_r}\left(\sum_{s=0}^{n_{\max}}L_{B_s} + \sum_{s=0}^{n_{\max}}L_{D_s}\right) \\ & + k_{p_3}L_{D_r}\left(\sum_{s=0}^{n_{\max}}L_{C_s} + R_S + R_0\right) + \frac{1}{2}k_t\sum_{s=1}^rL_{C_s}L_{C_{r-s}} \end{aligned} \quad (17)$$

Equations 1–17 were numerically integrated in Scilab through the algorithm ode. The concentration of cross-linked units, [CL]; total units, [U]; styrene units, [U₁]; and DVB units, [U₂] are equated in eqs 18, 19, 20, and 21, respectively.

$$[CL] = M_{2,0} - M_2 - PDB \quad (18)$$

$$[U] = [U_1] + [U_2] \quad (19)$$

$$[U_1] = M_{1,0} - M_1 \quad (20)$$

$$[U_2] = M_{2,0} - M_2 \quad (21)$$

2.4. Accessibility to Catalytic Sites. The fraction of inaccessible catalytic sites, Y_{ISU} , was used to calculate the effective ion exchange capacity (IEC_{eff}), i.e., the content of catalytic sites that are available for catalysis (eq 22).

$$IEC_{\text{eff}} = IEC(1 - Y_{ISU}) \quad (22)$$

The term IEC in eq 22 is a property of the resin which can be collected from the resin supplier or in literature studies (see Results and Discussion section).

It was assumed that the fraction of inaccessible sulfonated units relative to all sulfonated units is equal to the fraction of inaccessible total units relative to all units (eq 23).

$$Y_{ISU} = \frac{[ISU]}{[SU]} = \frac{[IU]}{[U]} \quad (23)$$

The fraction of cross-linked units is defined in eq 24.

$$Y_{CL} = \frac{[CL]}{[U]} \quad (24)$$

The fraction of $L_{E,n}$ sequences (containing n units) relative to all L_E sequences is described in eq 26.

$$Y_{LE,n} = \frac{L_{E,n}}{\sum_{j=1}^{n_{\max}}L_{Ej}} \quad (25)$$

2.5. Cross-Link Density. In the present work, the definition from Karam and Tien (1985)²⁰ was adopted for the cross-link density, which is represented by the molecular weight between cross-links. In the model developed herein, the average molecular weight between cross-links (\overline{M}_C) was estimated by eq 26.

$$\overline{M}_C = \frac{\overline{M}_U}{Y_{CL}} \quad (26)$$

where

$$\overline{M}_U = \frac{104.15U_1 + 130.19U_2}{U_1 + U_2} \quad (27)$$

The \overline{M}_C obtained from experimental data was calculated through the following nonlinear system of equations.²⁰

$$\ln(1 - v_R) + v_R + \mu_R v_R^2 + \frac{\rho_R V_1 v_R^{1/3}}{M_C K^{4/3}} - [\ln(1 - v_0) + v_0 + \mu_P v_0^2] = 0 \quad (28)$$

$$\ln(1 - v_R) + v_R + \mu_R v_R^2 + \frac{\rho_R V_1 v_R^{1/3}(1 + 2K^2)}{3\overline{M}_C K^{4/3}} + \frac{(K + 1)^3 + 2K^3}{2[(K + 1)^3 - K^3]} \{ \ln(1 - v_P) + v_P + \mu_P v_P^2 - [\ln(1 - v_0) + v_0 + \mu_P v_0^2] \} \quad (29)$$

$$K = \frac{v_R}{v_P} \quad (30)$$

$$SI = 1 + \frac{\left[\frac{\rho_S}{\rho_R} w_R \left(\frac{1}{v_R} - 1 \right) + \frac{\rho_S}{\rho_P} w_P \left(\frac{1}{v_P} - 1 \right) \right]}{w_R + w_P} \quad (31)$$

The system was fed with the experimental value of SI, $v_0 = 0$, and the parameters μ_P , μ_R , V_1 , ρ_R , ρ_S , and ρ_P , which are related in the Results and Discussion section. The occluded phase was neglected in the calculations ($w_P = 10^{-5}$ g and $w_R = 0.99999$ g were considered). The four equations and four unknowns, v_R , v_P , K , and M_C , were solved through a literature algorithm.²⁰

2.6. Model for Catalytic Reaction. Reversible resin-catalyzed reactions in the form $aA + bB \rightleftharpoons cC + dD$ were studied, where the limiting reagent was represented by A. The assumptions considered in the catalysis model were

1. Pseudohomogeneous (PH) approach;
2. Ideal mixture;
3. The equilibrium conversion was considered to be the highest conversion value obtained for the reaction studied (in general, the last conversion dots constitute a plateau);
4. Catalytic sites are equally distributed through the resin particles;
5. Noncatalyzed reaction rates were neglected.

Most of the catalyzed reactions studied herein are esterifications, where the reagents (A and B) are alcohol and acid, and the products (C and D) are ester and water.

The following set of equations was written for this part of the model:

$$\frac{dC_A}{dt} = -(-r_A) \quad (32)$$

$$-r_A = kC_{Cat}IEC_{eff} \left(C_A C_B - \frac{C_C C_D}{K_{eq}} \right) \quad (33)$$

$$C_B = C_{A0} \left(\theta_B - \frac{b}{a} X_A \right) \quad (34)$$

$$C_C = C_{A0} \left(\theta_C + \frac{c}{a} X_A \right) \quad (35)$$

$$C_D = C_{A0} \left(\theta_D + \frac{d}{a} X_A \right) \quad (36)$$

$$X_A = \frac{C_{A0} - C_A}{C_{A0}} \quad (37)$$

$$\theta_i = \frac{C_{i0}}{C_{A0}} \quad (\text{for } i = B, C, D) \quad (38)$$

Considering eqs 32–38, one can assert that this model can be applied to reversible resin-catalyzed reactions, and any degree of irreversibility would be tolerable (e.g., $K_{eq} \rightarrow \infty$).

In the case of mass transfer limitations, obtaining reaction rates requires more detailed treatment as shown elsewhere.²¹

The equilibrium constant (K_{eq}) was calculated based on the equilibrium conversion (third assumption). This simplified catalysis model was adopted in order to assess the effect of cross-link density on the accessibility of catalytic sites, avoiding complexities such as adsorption/desorption steps. The rate constant k from eq 33 refers to the reaction catalyzed by SO_3H , regardless of the type of resin which contains this group. Additionally, the accessibility reduction due to the polymer network characteristics of a given resin is taken into account in the term IEC_{eff} .

3. RESULTS AND DISCUSSION

Preliminary simulations were carried out with the copolymerization model in order to identify the value of n_{ax} (number of monomeric units in the longest sequence considered in the model) and assess cross-link density predictions. Table 3 shows the kinetic parameters used in the simulations.

Since the procedures to produce commercial resins are classified information, a study which reports the synthesis of sulfonated resins with different DVB contents was chosen as base for the copolymerization simulation.²² In the aforementioned study, sulfonated resins with similar features in relation to commercial resins were conceived. Then, the conditions reported in the referred work (1% benzoyl peroxide, 150% dilution, and 90 °C for 30 h) were used in the copolymerization simulations of the present study.

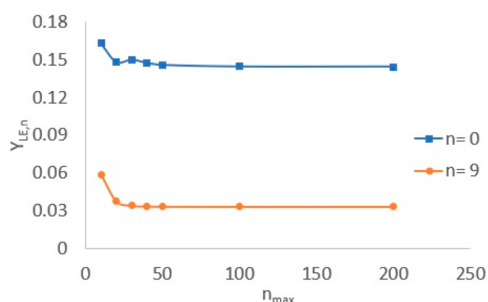
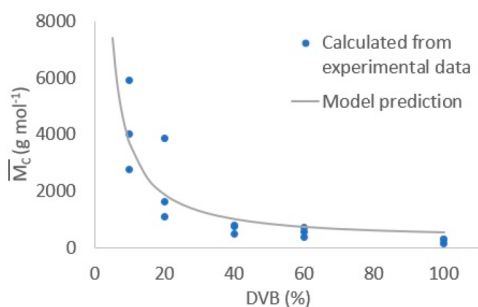
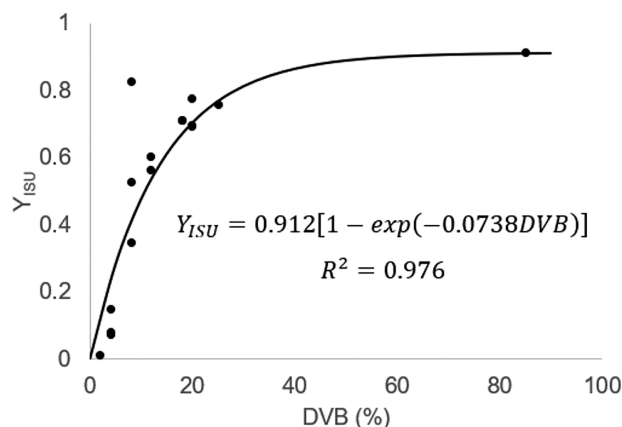
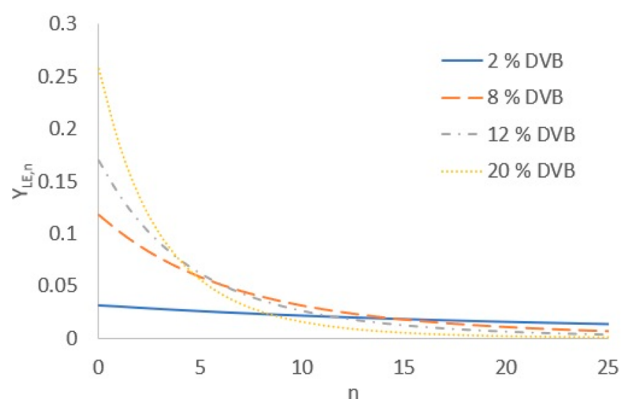
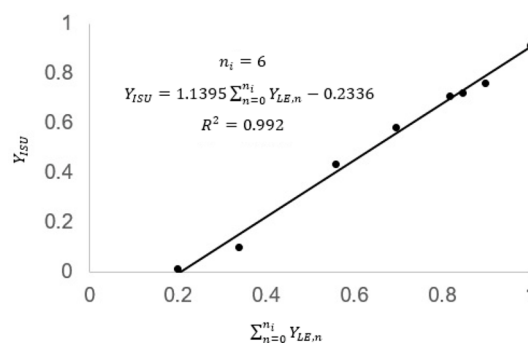
Simulations with different values of n_{max} were conducted in order to find a range where $Y_{LE,n}$ becomes constant. Figure 2 shows these simulations for $n = 0$ and 9.

It can be observed that there is not a considerable difference in $Y_{LE,n}$ for $n_{max} = 100$ and 200. Thus, $n_{max} = 100$ was adopted for all simulations.

Figure 3 shows a comparison between the \overline{M}_C estimated in the model and \overline{M}_C calculated from literature SI data (swelling experiments in toluene).²²

Table 3. Copolymerization Kinetic Parameters^a

rate constant	unit
$k_d = 6.94 \times 10^{13} \exp\left(-\frac{14710}{T}\right); f = 0.55$	s^{-1}
$k_{P_{11}} = 4.27 \times 10^7 \exp\left(-\frac{3909}{T}\right)$	$L \text{ mol}^{-1} s^{-1}$
$r_{1mDVB} = 0.43; r_{1pDVB} = 0.24$	
$k_{P_{12}} = \frac{k_{P_{11}}}{0.7r_{1mDVB} + 0.24r_{1pDVB}}$	$L \text{ mol}^{-1} s^{-1}$
$k_{P_{21}} = 0.77k_{P_{11}}; k_{P_{22}} = 0.77k_{P_{12}}$	$L \text{ mol}^{-1} s^{-1}$
$k_{P_1} = \frac{(U_1k_{P_{11}} + U_2k_{P_{21}})}{U_1 + U_2}$	$L \text{ mol}^{-1} s^{-1}$
$k_{P_2} = \frac{(U_1k_{P_{12}} + U_2k_{P_{22}})}{U_1 + U_2}$	$L \text{ mol}^{-1} s^{-1}$
$k_{t_1} = k_{P_{11}}; k_{t_2} = k_{P_{12}}$	$L \text{ mol}^{-1} s^{-1}$
$C_p = 0.2$	
$k_t = \left(\frac{k_{P_1}}{426.4 \exp\left(-\frac{3127}{T}\right)}\right)^2$	$L \text{ mol}^{-1} s^{-1}$
$k_{P_{1mPDB}} = \frac{C_p k_{P_{11}}}{2r_{1mDVB}}; k_{P_{1pPDB}} = \frac{C_p k_{P_{11}}}{2r_{1pDVB}}$	$L \text{ mol}^{-1} s^{-1}$
$k_{P_{2mPDB}} = 0.77k_{P_{1mPDB}}; k_{P_{2pPDB}} = 0.77k_{P_{1pPDB}}$	$L \text{ mol}^{-1} s^{-1}$
$k_{P_{13}} = 0.7 k_{P_{1mPDB}} + 0.3 k_{P_{1pPDB}}$	$L \text{ mol}^{-1} s^{-1}$
$k_{P_{23}} = 0.7 k_{P_{2mPDB}} + 0.3 k_{P_{2pPDB}}$	$L \text{ mol}^{-1} s^{-1}$
$k_{P_3} = \frac{(U_1k_{P_{13}} + U_2k_{P_{23}})}{U_1 + U_2}$	$L \text{ mol}^{-1} s^{-1}$

^aData collected from ref 15.Figure 2. Determination of the number of monomeric units in the longest sequence to be considered in the model (n_{max}). Simulation conducted for 10% DVB.Figure 3. Cross-link density predictions (from eq 26). $\mu_p = 0.3527, \mu_R = 0.3975, V_1 = 106.2745 \text{ mL mol}^{-1}, \rho_R = 1.1 \text{ g mL}^{-1}, \rho_S = 0.867 \text{ g mL}^{-1}$, and $\rho_p = 1.005 \text{ g mL}^{-1}$.Figure 4. Correlation between Y_{ISU} and DVB content in the resins.Figure 5. $Y_{LE,n}$ distribution.Figure 6. Y_{ISU} linear correlation.

An acceptable fitting is observed in Figure 3, indicating that the copolymerization model simulated with literature parameters (Table 3) constitutes a reasonable approach to represent the cross-linking degree of styrene–DVB resins.

Data from 14 studies on catalysis involving several sulfonated styrene–DVB resins were collected. Studies involving reaction characteristics that are far from the domain of this work, such as oil esterification (multiple reactions) and the use of surface sulfonated resins (e.g., Amberlyst 46), were not included in the analysis. Tables S1 and S2^{28–47} present the resins properties and the catalyzed reaction conditions, respectively.

After the second-order PH model is applied to the reaction conditions reported in Table S2, the results shown in Figure S1 and S2 are achieved. In these simulations, the fitting parameters were the fraction of inaccessible sulfonated units (Y_{ISU}) and the

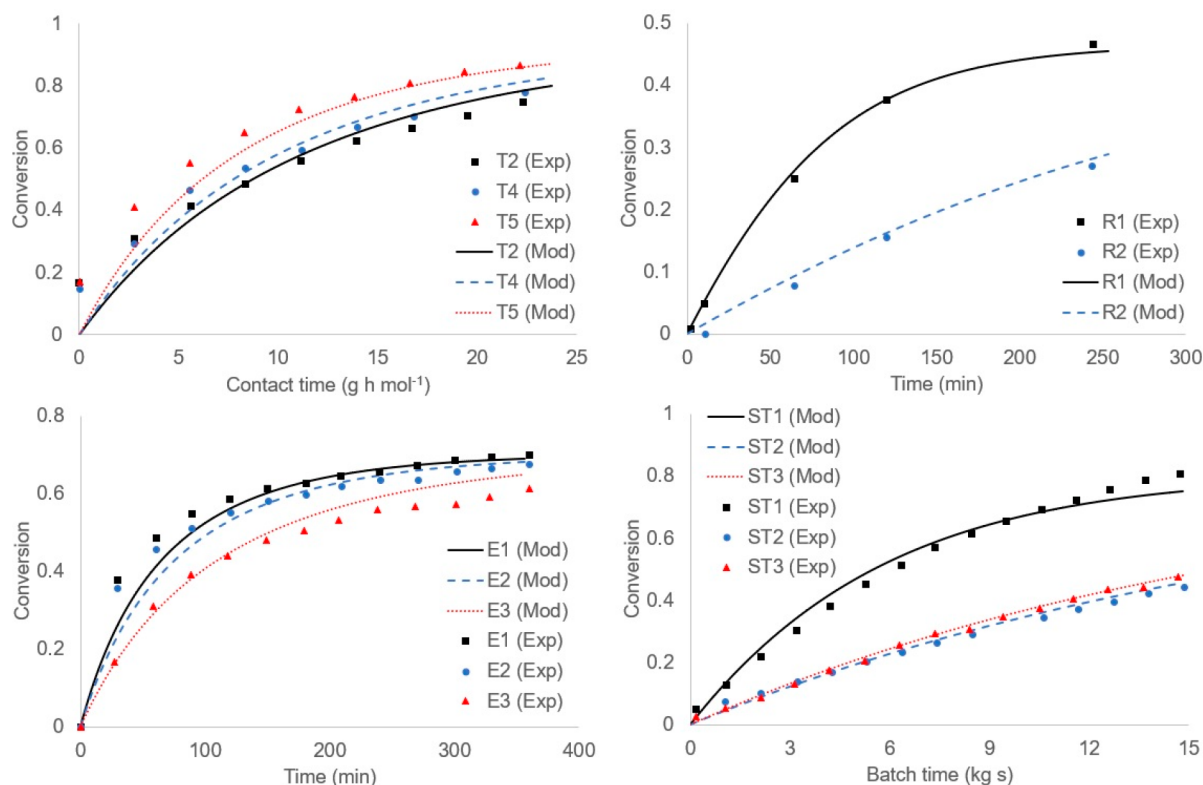


Figure 7. Fittings obtained with eq 37 ($\alpha = 1.1395$, $\beta = 0.2336$) and the same k values from Table S2.

rate constant of each reaction catalyzed by SO_3H (k), both reported in Table S2. Good agreements between experimental data and model predictions can be observed in the aforementioned figures. Nonetheless, the k values fitted in the present work were higher than those fitted in literature studies for the same reaction and conditions. This is an expected result, since the constant k found in this study represents the effective rate constant of the SO_3H -catalyzed reaction, while the constant k calculated in most literature is underestimated due to the hindering effect in the resin. The following average k values obtained for resin-catalyzed reactions from literature can be cited: 9.5×10^{-5} ,³⁴ 3.4×10^{-5} ,⁴¹ 1.2×10^{-4} ,³⁸ and 4.9×10^{-5} ,⁴⁸ and the respective SO_3H -catalyzed rate constants obtained in this work (Table S2): 1.1×10^{-4} , 5.0×10^{-5} , 4.0×10^{-4} , and 9.0×10^{-5} (all in $\text{L}^2 \text{mol}^{-2} \text{s}$).

The fitted Y_{ISU} values are consistent with the resin's degree of cross-linking; i.e., higher Y_{ISU} values were found for resins with higher degrees of cross-linking.

It can be stated that Y_{ISU} depends not only on the cross-linking degree of the resin but also on the molecular size of the compounds involved in the catalyzed reaction. However, as an average approach, a mean Y_{ISU} was calculated for each resin by using information from Table S2. Despite the effect of other process variables on Y_{ISU} , a correlation of this parameter with the DVB percentage could be verified and is depicted in Figure 4.

The outlier observed in Figure 4 ($Y_{\text{ISU}} \cong 0.82$) refers to the resin Amberlite IR120. In spite of the relatively low DVB content (8%), this resin presents the lowest volume of pores among the resins related in Table S1 ($V_{\text{Pores}} = 0.011 \text{ cm}^3 \text{ g}^{-1}$). The higher average Y_{ISU} obtained for this resin can be attributed to the additional hindering effect caused by its low porosity. Hence, the exponential fit (with $R^2 = 0.976$) was adjusted disregarding the dot referred to in AIR120.

From the copolymerization model, higher fractions of $Y_{\text{LE},n}$ are obtained for higher DVB contents in the range of small values of n (0–10), as expected (Figure 5). One can assert that the hindering effect will be more significant around cross-linked units connected by smaller numbers of units. Figure 5 indicates that, working with a given n in the range 0–10, it is possible to mathematically represent the effect of cross-link density on the accessibility of catalytic sites in the resin due to the sharp variations of n in comparison with the behavior observed for higher n values ($n > 10$).

In order to introduce a predictive feature in the present approach, Y_{ISU} was assumed to be directly proportional to the fraction of inaccessible cross-linked units in the resin, $\sum_{n=0}^{n_i} Y_{\text{LE},n}$ where n_i is the maximum number of units between cross-links for occurring hindering effects (i.e., for $n > n_i$, $Y_{\text{LE},n}$ does not consist of inaccessible cross-linked units). In other words, the criterion adopted to consider a site inaccessible would be that it is near two cross-linked units connected by n_i or less units, and the fraction of inaccessible sites would have a linear correlation with $\sum_{n=0}^{n_i} Y_{\text{LE},n}$ as proposed in eq 39.

$$Y_{\text{ISU}} = \alpha \sum_{n=0}^{n_i} Y_{\text{LE},n} + \beta \quad (39)$$

Equation 39 was fitted with values of Y_{ISU} and $\sum_{n=0}^{n_i} Y_{\text{LE},n}$ obtained in the present work. The Y_{ISU} was determined for each studied DVB percentage. Average Y_{ISU} values were calculated from Figure 4 for DVB contents of 2, 4, 8, 12, 18, 20, 25, and 85%. The respective $\sum_{n=0}^{n_i} Y_{\text{LE},n}$ values were calculated first for $n_i = 0$. This fitting procedure was repeated for $n_i = 1, 2, \dots, 10$, since the range $n = 0$ –10 proved to be adequate according to Figure 5. The best fitting result occurred for $n_i = 6$, which provided $R^2 = 0.992$, as shown in Figure 6.

As already mentioned, this modeling study is an average approach, since catalytic efficiency depends not only on the cross-linking degree but also on system variables such as swelling index, molecular size of reaction components, and partition coefficients, among others. Nevertheless, the correlation proposed in eq 39 (determined in Figure 6) is still valid for several literature cases that are close to this linear average behavior, as demonstrated in Figure 7.

Reasonable fittings are verified in Figure 7, which confirm the applicability of eq 39 in modeling reactions (mostly esterifications) catalyzed by sulfonated resins with many similar characteristics, except for the degree of cross-linking.

The present modeling approach can be refined by validating eq 39 through experiments with less variations: the same reaction for all runs and sulfonated resins synthesized under the same conditions, except DVB content (i.e., isolating the effect of cross-linking degree on the catalytic activity).

4. CONCLUSION

A mathematical approach comprised of copolymerization and resin-catalyzed reactions was developed and validated with literature data. A maximum of 100 monomer units proved sufficient for the sequences approach applied to the styrene/DVB copolymerization. The copolymerization model was able to represent the trend of cross-link density as a function of DVB content, which was confirmed by calculations from swelling index experimental data. The rate constants found for the SO_3H -catalyzed reactions are above the literature values, demonstrating that the hindering effect can be separated from this parameter. The fraction of inaccessible catalytic sites presented a large range showing values of about 10% (for 4% DVB resins) and 72% (for 20% DVB resins). On average, the fraction of inaccessible sulfonated units followed an exponential profile as a function of DVB percentage and a linear correlation with the fraction of inaccessible cross-links. Based on this linear correlation, it can be concluded that inaccessible cross-links are connected by, at most, six monomer units. This finding is corroborated by the $L_{E,n}$ sequences distribution provided by the copolymerization model, which points out that the main differences between resins with distinct DVB contents occur when considering sequences connected by 0–10 monomer units. In summary, the effect of cross-link density on the resin-catalyzed reactions can be quantified through the use of polymerization modeling tools, which provide a wealth of information on the polymer network that constitutes the resin.

■ ASSOCIATED CONTENT

Supporting Information

The Supporting Information is available free of charge at <https://pubs.acs.org/doi/10.1021/acs.iecr.1c00695>.

Tables S1 and S2; Figures S1 and S2 (PDF)

■ AUTHOR INFORMATION

Corresponding Author

Leandro G. Aguiar – Departamento de Engenharia Química, Escola de Engenharia de Lorena, Universidade de São Paulo, 12602-810 Lorena, SP, Brazil; orcid.org/0000-0002-2055-9317; Email: leandroaguiar@usp.br

Authors

William M. Godoy – Departamento de Engenharia Química, Escola de Engenharia de Lorena, Universidade de São Paulo,

12602-810 Lorena, SP, Brazil; orcid.org/0000-0002-0088-3726

Leonardo Nápolis – Departamento de Engenharia Química, Escola de Engenharia de Lorena, Universidade de São Paulo, 12602-810 Lorena, SP, Brazil

Rui P. V. Faria – LSRE–Faculdade de Engenharia da Universidade do Porto, 4200-456 Porto, Portugal; orcid.org/0000-0002-1216-0613

Alírio E. Rodrigues – LSRE–Faculdade de Engenharia da Universidade do Porto, 4200-456 Porto, Portugal; orcid.org/0000-0002-0715-4761

Complete contact information is available at: <https://pubs.acs.org/10.1021/acs.iecr.1c00695>

Notes

The authors declare no competing financial interest.

■ ACKNOWLEDGMENTS

The authors are grateful to FAPESP (process 2017/26985-4) and CAPES (Finance code: 001) for the financial support.

■ ACRONYMS

CL = cross-linked unit
 DVB = divinylbenzene
 F = polymer fragment
 IEC = ion exchange capacity
 IU = inaccessible units
 ISU = inaccessible sulfonated unit
 P = dead polymer
 PDB = pendant double bond
 r.u. = repeating units
 SU = sulfonated unit
 U = polymerized unit

Symbology

symbol = description, unit
 C_{a0} = initial concentration of the component a , mol L⁻¹
 C_i = concentration of the component i , mol L⁻¹
 C_{i0} = initial concentration of the component i , mol L⁻¹
 C_{HCl} = concentration of HCl solution, mol L⁻¹
 C_p = reactivity correlation parameter, dimensionless
 $[\text{CL}]$ = cross-linked units concentration, mol L⁻¹
 f = initiator efficiency, dimensionless
 I = initiator concentration, mol L⁻¹
 IEC = ion exchange capacity, meq g⁻¹
 IEC_{eff} = effective ion exchange capacity, mequiv g⁻¹
 $[\text{ISU}]$ = concentration of inaccessible sulfonated units, mol L⁻¹
 $[\text{IU}]$ = concentration of inaccessible units, mol L⁻¹
 k = rate constant of the reaction catalyzed by SO_3H , L² mol⁻² min⁻¹
 K = ratio $\frac{v_R}{v_p}$, dimensionless
 k_d = initiator decomposition constant, s⁻¹
 k_{eq} = equilibrium constant, dimensionless
 k_{i1} = styrene initiation constant, L mol⁻¹ s⁻¹
 k_{i2} = DVB initiation constant, L mol⁻¹ s⁻¹
 k_{p1} = styrene propagation constant, L mol⁻¹ s⁻¹
 k_{p2} = DVB propagation constant, L mol⁻¹ s⁻¹
 k_{p3} = PDB propagation constant, L mol⁻¹ s⁻¹
 k_t = termination constant, L mol⁻¹ s⁻¹
 L_A = concentrations of sequences containing r styrene units connecting a PDB to a radical center, mol L⁻¹

L_{B_r} = concentration of sequences containing r styrene units connecting two PDBs, mol L⁻¹

L_{C_r} = concentration of sequences containing r styrene units connecting a cross-linked unit to a radical center, mol L⁻¹

L_{D_r} = concentration of sequences containing r styrene units connecting a PDB to a cross-linked unit, mol L⁻¹

L_{E_r} = concentration of sequences containing r styrene units connecting two cross-linked units, mol L⁻¹

M_1 = styrene concentration, mol L⁻¹

$M_{1,0}$ = initial styrene concentration, mol L⁻¹

M_2 = DVB concentration, mol L⁻¹

$M_{2,0}$ = initial DVB concentration, mol L⁻¹

\overline{M}_C = average molecular weight between CLs, g mol⁻¹

\overline{M}_U = average molecular weight of polymerized units, g mol⁻¹

n = number of units between CLs, r.u.

n_i = maximum n considered for inaccessible CLs, r.u.

n_{\max} = maximum n considered in the copolymerization modeling, r.u.

PDB = pendant double bonds concentration, mol L⁻¹

R' = total radicals' concentration, mol L⁻¹

R'_0 = primary radicals' concentration, mol L⁻¹

$-r_A$ = rate of consumption of A, mol L⁻¹ min⁻¹

R'_S = concentration of radicals containing only styrene units, mol L⁻¹

SI = swelling index, dimensionless

[SU] = concentration of sulfonated units, mol L⁻¹

[U] = concentration of total polymerized units, mol L⁻¹

[U₁] = concentration of styrene units, mol L⁻¹

[U₂] = concentration of DVB units, mol L⁻¹

v_0 = volume fraction of dissolved polymer in the supernate, dimensionless

V_1 = molar volume of solvent, cm³ mol⁻¹

v_P = volume fraction of polystyrene in the swollen occluded polystyrene, dimensionless

v_R = volume fraction of rubber in the swollen rubber network, dimensionless

W_d = mass of dry resin, g

w_P = weight of occluded polystyrene in the gel, g

w_R = weight of rubber in the gel, g

X_A = conversion of A, dimensionless

Y_{CL} = fraction of cross-linked units, mol CL (mol U)⁻¹

$Y_{LE,n}$ = fraction of $L_{E,n}$ among all $L_{E,r}$, mol $L_{E,n}$ (mol total L_E)⁻¹

Y_{ISU} = fraction of inaccessible sulfonated units, mol ISU (mol SU)⁻¹

θ_i = feed ratio between excess and limiting reagents, dimensionless

μ_R = rubber–solvent interaction factor, dimensionless

μ_P = polystyrene–solvent interaction factor, dimensionless

ρ_P = density of the polystyrene, g cm⁻³

ρ_R = density of the rubber, g cm⁻³

ρ_S = density of the solvent, g cm⁻³

REFERENCES

- Casas, C.; Bringué, R.; Ramírez, E.; Iborra, M.; Tejero, J. Liquid-Phase Dehydration of 1-Octanol, 1-Hexanol and 1-Pentanol to Linear Symmetrical Ethers over Ion Exchange Resins. *Appl. Catal., A* **2011**, *396* (1–2), 129–139.
- Russo, V.; Tesser, R.; Rossano, C.; Cogliano, T.; Vitiello, R.; Leveur, S.; Di Serio, M. Kinetic Study of Amberlite IR120 Catalyzed Acid Esterification of Levulinic Acid with Ethanol: From Batch to Continuous Operation. *Chem. Eng. J.* **2020**, *401* (June), 126126.
- Granollers, M.; Izquierdo, J. F.; Cunill, F. Effect of Macroreticular Acidic Ion-Exchange Resins on 2-Methyl-1-Butene and 2-Methyl-2-

Butene Mixture Oligomerization. *Appl. Catal., A* **2012**, *435–436*, 163–171.

(4) Badia, J. H.; Fité, C.; Bringué, R.; Iborra, M.; Cunill, F. Catalytic Activity and Accessibility of Acidic Ion-Exchange Resins in Liquid Phase Etherification Reactions. *Top. Catal.* **2015**, *58* (14–17), 919–932.

(5) Tejero, M. A.; Ramírez, E.; Fité, C.; Tejero, J.; Cunill, F. Esterification of Levulinic Acid with Butanol over Ion Exchange Resins. *Appl. Catal., A* **2016**, *517*, 56–66.

(6) Vil', V. A.; Yaremenko, I. A.; Fomenkov, D. I.; Levitsky, D. O.; Fleury, F.; Terent'ev, A. O. Ion Exchange Resin-Catalyzed Synthesis of Bridged Tetraoxanes Possessing in Vitro Cytotoxicity against HeLa Cancer Cells. *Chem. Heterocycl. Compd.* **2020**, *56* (6), 722–726.

(7) Penariol, J. L.; Theodoro, T. R.; Dias, J. R.; Carpegiani, J. A.; Aguiar, L. G. Application of a Sulfonated Styrene-(Ethylene Glycol Dimethacrylate) Resin as Catalyst. *Kinet. Catal.* **2019**, *60* (5), 650–653.

(8) Carpegiani, J. A.; Godoy, W. M.; Guimaraes, D. H. P.; Aguiar, L. G. Glycerol Acetylation Catalyzed by an Acidic Styrene-Co-Dimethacrylate Resin: Experiments and Kinetic Modeling. *React. Kinet., Mech. Catal.* **2020**, *130* (1), 447–461.

(9) Silva, V. F. L.; Penariol, J. L.; Dias, J. R.; Theodoro, T. R.; Carpegiani, J. A.; Aguiar, L. G. Sulfonated Styrene-Dimethacrylate Resins with Improved Catalytic Activity. *Kinet. Catal.* **2019**, *60* (5), 654.

(10) Rodriguez, O.; Setínek, K. Dependence of Esterification Rates on Crosslinking of Ion Exchange Resins Used as Solid Catalysts. *J. Catal.* **1975**, *39* (3), 449–455.

(11) Jerabek, K.; Setínek, K. Polymer Matrix Influence on Ion Exchange Resin-Catalyzed Reactions. *J. Mol. Catal.* **1987**, *39* (2), 161–167.

(12) Aguiar, L. G.; Gonçalves, M. A. D.; Pinto, V. D.; Dias, R. C. S.; Costa, M. R. P. F. N.; Giudici, R. Development of Cyclic Propagation Kinetics for Modeling the Nitroxide-Mediated Radical Copolymerization of Styrene-Divinylbenzene. *Macromol. React. Eng.* **2014**, *8* (4), 282.

(13) López-Domínguez, P.; Hernández-Ortiz, J. C.; Vivaldo-Lima, E. Modeling of RAFT Copolymerization with Crosslinking of Styrene/Divinylbenzene in Supercritical Carbon Dioxide. *Macromol. Theory Simul.* **2018**, *27* (1), 1700064.

(14) Aguiar, L. G.; Moura, J. O. V.; Theodoro, T. R.; Neto, T. G. S.; Lopes, V. M. P.; Dias, J. R. Prediction of Resin Textural Properties by Vinyl/Divinyl Copolymerization Modeling. *Polymer* **2017**, *129*, 21.

(15) Aguiar, L. G.; Gonçalves, M. A. D.; Pinto, V. D.; Dias, R. C. S.; Costa, M. R. P. F. N.; Giudici, R. Mathematical Modeling of NMRP of Styrene-Divinylbenzene over the Pre- and Post-Gelation Periods Including Cyclization. *Macromol. React. Eng.* **2014**, *8* (4), 295.

(16) Bringué, R.; Ramírez, E.; Iborra, M.; Tejero, J.; Cunill, F. Esterification of Furfuryl Alcohol to Butyl Levulinate over Ion-Exchange Resins. *Fuel* **2019**, *257*, 116010.

(17) Theodoro, T. R.; Dias, J. R.; Penariol, J. L.; Moura, J. O. V.; Aguiar, L. G. Sulfonated Poly (Styrene-Co-Ethylene Glycol Dimethacrylate) with Attractive Ion Exchange Capacity. *Polym. Adv. Technol.* **2018**, *29*, 2759–2765.

(18) Storey, B. T. Copolymerization of Styrene and P-Divinylbenzene. Initial Rates and Gel Points. *J. Polym. Sci., Part A: Gen. Pap.* **1965**, *3* (1), 265–282.

(19) Aguiar, L. G.; Gonçalves, M. A. D.; Pinto, V. D.; Dias, R. C. S.; Costa, M. R. P. F. N.; Giudici, R. Development of Cyclic Propagation Kinetics for Modeling the Nitroxide-Mediated Radical Copolymerization of Styrene-Divinylbenzene. *Macromol. React. Eng.* **2014**, *8* (4), 282–294.

(20) Karam, H. J.; Tien, L. Analysis of Swelling of Crosslinked Rubber Gel with Occlusions. *J. Appl. Polym. Sci.* **1985**, *30* (5), 1969–1988.

(21) Silva, V. M. T. M.; Rodrigues, A. E. Kinetic Studies in a Batch Reactor Using Ion Exchange Resin Catalysts for Oxygenates Production: Role of Mass Transfer Mechanisms. *Chem. Eng. Sci.* **2006**, *61* (2), 316–331.

(22) Coutinho, F. M. B.; Rezende, S. M.; Soares, B. G. Characterization of Sulfonated Poly (Styrene-Divinylbenzene) and Poly-(Divinylbenzene) and Its Application as Catalysts in Esterification Reaction. *J. Appl. Polym. Sci.* **2006**, *102* (4), 3616–3627.

- (23) Okay, O. Styrene-Divinylbenzene Copolymers *. *Angew. Makromol. Chem.* **1988**, *157* (2594), 1–13.
- (24) Mori, S. Elution Behavior of Some Solutes on a Porous Polystyrene Gel in High Performance Liquid Chromatography. *Anal. Chem.* **1978**, *50* (6), 745–748.
- (25) Mieczkowski, R. The Determination of the Solubility Parameter Components of Polystyrene by Partial Specific Volume Measurements. *Eur. Polym. J.* **1988**, *24* (12), 1185–1189.
- (26) García, M. T.; Gracia, I.; Duque, G.; Lucas, A. d.; Rodriguez, J. F. Study of the Solubility and Stability of Polystyrene Wastes in a Dissolution Recycling Process. *Waste Manage.* **2009**, *29* (6), 1814–1818.
- (27) Errede, L. A. Polymer Swelling. 5. Correlation of Relative Swelling of Poly(Styrene-Co-Divinylbenzene) with the Hildebrand Solubility Parameter of the Swelling Liquid. *Macromolecules* **1986**, *19* (6), 1522–1525.
- (28) Guilera, J.; Ramírez, E.; Fité, C.; Tejero, J.; Cunill, F. Synthesis of Ethyl Hexyl Ether over Acidic Ion-Exchange Resins for Cleaner Diesel Fuel. *Catal. Sci. Technol.* **2015**, *5* (4), 2238–2250.
- (29) Iborra, M.; Tejero, J.; Cunill, F.; Izquierdo, J. F.; Fité, C. Drying of Acidic Macroporous Styrene-Divinylbenzene Resins with 12–20% Cross-Linking Degree. *Ind. Eng. Chem. Res.* **2000**, *39* (5), 1416–1422.
- (30) Pitochelli, A. R. Ion Exchange Catalysis and Matrix Effects. *J. Chem. Eng. Process Technol.* **2014**, *05*, 1–36.
- (31) Dixit, A. B.; Yadav, G. D. Deactivation of Ion-Exchange Resin Catalysts. Part I: Alkylation of *o*-Xylene with Styrene. *React. Funct. Polym.* **1996**, *31* (3), 237–250.
- (32) Dos Reis, S. C. M.; Lachter, E. R.; Nascimento, R. S. V.; Rodrigues, J. A.; Reid, M. G. Transesterification of Brazilian Vegetable Oils with Methanol over Ion-Exchange Resins. *J. Am. Oil Chem. Soc.* **2005**, *82* (9), 661–665.
- (33) Komoń, T.; Niewiadomski, P.; Oracz, P.; Jamróz, M. E. Esterification of Acrylic Acid with 2-Ethylhexan-1-ol: Thermodynamic and Kinetic Study. *Appl. Catal., A* **2013**, *451*, 127–136.
- (34) Patwardhan, A. A.; Sharma, M. M. Esterification of Carboxylic Acids with Olefins Using Cation Exchange Resins as Catalysts. *React. Polym.* **1990**, *13* (1–2), 161–176.
- (35) Çitak, A. Application of Ion Exchange Resins in the Synthesis of Isobutyl Acetate. *Ion Exchange Technology II: Applications* **2012**, 137–148.
- (36) Ali, S. H.; Merchant, S. Q. Kinetic Study of Dowex 50 Wx8-Catalyzed Esterification and Hydrolysis of Benzyl Acetate. *Ind. Eng. Chem. Res.* **2009**, *48* (5), 2519–2532.
- (37) Dosuna-Rodríguez, I.; Gaigneaux, E. M. Glycerol Acetylation Catalysed by Ion Exchange Resins. *Catal. Today* **2012**, *195* (1), 14–21.
- (38) Chakrabarti, A.; Sharma, M. M. Esterification of Acetic Acid with Styrene: Ion Exchange Resins as Catalysts. *React. Polym.* **1991**, *16* (1), 51–59.
- (39) Van de Steene, E.; De Clercq, J.; Thybaut, J. W. Ion-Exchange Resin Catalyzed Transesterification of Ethyl Acetate with Methanol: Gel versus Macroporous Resins. *Chem. Eng. J.* **2014**, *242*, 170–179.
- (40) Izci, A.; Bodur, F. Liquid-Phase Esterification of Acetic Acid with Isobutanol Catalyzed by Ion-Exchange Resins. *React. Funct. Polym.* **2007**, *67* (12), 1458–1464.
- (41) Yadav, G. D.; Thathagar, M. B. Esterification of Maleic Acid with Ethanol over Cation-Exchange Resin Catalysts. *React. Funct. Polym.* **2002**, *52* (2), 99–110.
- (42) Sanz, M. T.; Murga, R.; Beltrán, S.; Cabezas, J. L.; Coca, J. Autocatalyzed and Ion-Exchange-Resin-Catalyzed Esterification Kinetics of Lactic Acid with Methanol. *Ind. Eng. Chem. Res.* **2002**, *41* (3), 512–517.
- (43) Rios, L. A.; Weckes, P. P.; Schuster, H.; Hoelderich, W. F. Resin Catalyzed Alcoholysis of Epoxidized Fatty Esters: Effect of the Alcohol and the Resin Structures. *Appl. Catal., A* **2005**, *284* (1–2), 155–161.
- (44) Gangadwala, J.; Mankar, S.; Mahajani, S.; Kienle, A.; Stein, E. Esterification of Acetic Acid with Butanol in the Presence of Ion-Exchange Resins as Catalysts. *Ind. Eng. Chem. Res.* **2003**, *42* (10), 2146–2155.
- (45) Yadav, G. D.; Kulkarni, H. B. Ion-Exchange Resin Catalysis in the Synthesis of Isopropyl Lactate. *React. Funct. Polym.* **2000**, *44* (2), 153–165.
- (46) Ali, S. H.; Merchant, S. Q. Kinetics of the Esterification of Acetic Acid with 2-Propanol: Impact of Different Acidic Cation Exchange Resins on Reaction Mechanism. *Int. J. Chem. Kinet.* **2006**, *38* (10), 593–612.
- (47) Yadav, G. D.; Rahuman, M. S. M. M. Activities of Clays and Ion Exchange Resins in the Synthesis of Phthalate Esters. *Clean Technol. Environ. Policy* **2004**, *6* (2), 114–119.
- (48) Erdem, B.; Cebe, M. Kinetics of Esterification of Propionic Acid with *N*-Amyl Alcohol in the Presence of Cation Exchange Resins. *Korean J. Chem. Eng.* **2006**, *23* (6), 896–901.